


Article

Spectral and Timing Properties of H 1743-322 in the “Faint” 2005 Normal Outburst

Aijun Dong ^{1,2} , Chang Liu ^{1,2,*}, Qijun Zhi ^{1,2}, Ziyi You ^{1,2}, Qibin Sun ^{1,2} and Bowen Du ^{1,2}
¹ School of Physics and Electronic Science, Guizhou Normal University, Guiyang 550025, China; Aijdong@gznu.edu.cn (A.D.); qjzhi@gznu.edu.cn (Q.Z.); 100232632@gznu.edu.cn (Z.Y.); sqb@gznu.edu.cn (Q.S.); bowen_du@gznu.edu.cn (B.D.)

² Guizhou Provincial Key Laboratory of Radio Astronomy and Data Processing, Guizhou Normal University, Guiyang 550025, China

* Correspondence: changliu@gznu.edu.cn

Abstract: H 1743-322 is a well-known black hole X-ray binary (BH XRBs) that has been observed in several outbursts over the past. In this work, we have performed the spectral and timing analysis of H 1743-322 during the “faint” 2005 outburst for the first time with the RXTE/PCA data. In this outburst, the spectral and timing parameters (e.g., T_{in} , Γ , R_{in} , rms and QPOs, etc.) presented an obvious change and a q-like pattern was found in the Hardness Intensity Diagram (HID), which often named as the hysteresis effect of BH XRBs. The radius of the innermost stable circular orbit was constrained as $R_{\text{ISCO}} \sim 3.50 R_g$, which predicts that H 1743-322 is a lower-spin black hole. We further explored the correlation between timing and spectral properties. The relation of photon index Γ and X-ray flux, $F_{3-25\text{keV}}$, presented a transition between negative and positive correlation when the X-ray luminosity, $L_{3-25\text{keV}}$, is above and below a critical X-ray luminosity, $L_{X,\text{crit}} \simeq 2.55 \times 10^{-3} L_{\text{Edd}}$, which can be well explained by the Shakura-Sunyaev disk–corona model (SSD-corona) and advection-dominated accretion flow (ADAF). We also found the tight linear, negative correlation between photon index Γ and the total fractional rms . Since the amount of soft photons from the accretion disk seems invariable, an increase of the number of soft photons will dilute the variability from the harder photons. Therefore, the softer the X-ray spectra will result in the smaller total fractional rms . The above results suggested that the 2005 outburst of H 1743-322 was a normal outburst and H 1743-322 represented similar properties with other black hole X-ray binaries.

Keywords: accretion; accretion disk; stars: black holes; X-ray binaries; X-rays: individual: H 1743-322



Citation: Dong, A.; Liu, C.; Zhi, Q.; You, Z.; Sun, Q.; Du, B. Spectral and Timing Properties of H 1743-322 in the “Faint” 2005 Normal Outburst. *Universe* **2022**, *8*, 273. <https://doi.org/10.3390/universe8050273>

Academic Editor: Luigi Foschini

Received: 7 April 2022

Accepted: 29 April 2022

Published: 6 May 2022

Publisher’s Note: MDPI stays neutral with regard to jurisdictional claims in published maps and institutional affiliations.



Copyright: © 2022 by the authors. Licensee MDPI, Basel, Switzerland. This article is an open access article distributed under the terms and conditions of the Creative Commons Attribution (CC BY) license (<https://creativecommons.org/licenses/by/4.0/>).

1. Introduction

Most of black hole X-ray binaries (BH XRBs) are transients, which can be observed in an outburst. During the outburst, the X-ray luminosity can increase several orders of magnitude to approach the Eddington luminosity ($L_{\text{Edd}} \simeq 1.3 \times 10^{38} (\frac{M_{\text{BH}}}{M_{\odot}}) \text{ erg} \cdot \text{s}^{-1}$) [1,2]. BH XRBs often display a q-like pattern in the hardness-intensity diagram (HID). The phenomena with the different X-ray luminosity at the same hardness ratio (HR) are often named as the hysteresis effects of BH XRBs. Based on their spectral and timing properties, several main spectral states can be identified: Low/Hard State (LHS), Intermediate State (IMS) and High/Soft State (HSS). The IMS are often divided into Hard Intermediate States (HIMS) and Soft Intermediate States (SIMS). Low Frequency Quasi-Periodic Oscillations (LFQPOs) are the most salient feature in the power density spectrum (PDS) of BH XRBs in the LHS and IMS, which can be divided into three different categories: type-A Quasi-Periodic Oscillations (type-A QPOs), type-B Quasi-Periodic Oscillations (type-B QPOs) and type-C Quasi-Periodic Oscillations (type-C QPOs) [3]. A typical outburst often starts with the LHS, where the X-ray spectra are dominated by the non-thermal power-law component extending to $\sim 100 \text{ keV}$ with the spectral index $1.5 \leq \Gamma \leq 2.0$. In LHS, the PDS sometimes exist with a type-C QPOs characterized by strong, narrow peak frequency with strong band-limited noise component ($rms \sim 30\%$) [4–8]. As the X-ray luminosity increases, XRBs

will enter into the IMS, where the disk is close to the innermost stable circular orbit (ISCO) or moderately truncated along with an optically thick, low-temperature corona in the inner region. In this state, both thermal and non-thermal components are very strong. The PDS in the IMS sometimes shows the type-A QPOs and type-B QPOs, which are characterized by the absence of a flat top noise [9,10]. Near the peak luminosity, the XRBs will enter into HSS, where the X-ray emission is dominated by thermal disk component with a high energy tail extending to 100 keV ($2.0 \leq \Gamma \leq 2.4$). Some outbursts of BH XRBs are called mini-outbursts, because they often happen soon after the X-ray flux close to the quiescent level and are of smaller amplitude and shorter duration compared with the normal outburst [11]. In recent year, more and more mini-outbursts were observed in several BH XRBs (e.g., GRS 1739-278, Swift J1753.5-0127 and XTE J1118+480) [12–14]. However, the physical mechanism of mini-outburst is still unclear. The main accretion models include the disk instability model [15] and the companion star radiation [16].

H 1743-322 is a BH X-ray transient that was first discovered by HEAO-1 and Ariel 5 in 1977 [17]. Since then, H 1743-322 remained in the quiescent state till 1984 when Reynolds reported X-ray activities by EXOSAT [18]. The brightest outburst of H 1743-322 was detected by Rossi X-ray Timing Explorer (RXTE) on March 20, 2003, the peak luminosity of which increased up to 1.3 Crab at 1.5–12 keV. Based on the observations of RXTE in 2003, Steiner et al. (2012) constrained the physical parameters of H 1743-322 with symmetric kinematic model and obtained the distance $D_L = 8.5 \pm 0.8$ kpc, inclination angle $i^0 = 75^\circ \pm 3.0^\circ$ [19]. Using the RXTE observations of H 1743-322 in 2004, Bhattacharjee et al. (2017) applied the Two Component Advective Flow (TCAF) solution to analyze the spectral and timing properties and constrained the range of BH mass $M_{BH} = 10.31M_\odot - 14.07M_\odot$ [20]. In 2008, H 1743-322 underwent another outburst where H 1743-322 showed a canonical q-like pattern in HID diagrams. A secondary outburst was detected by INTEGRAL, RXTE and Swift in 2008 and a transition between LHS and IMS was found. During this outburst, the smallest value of Hardness ratios was about 0.5, which predicted this outburst to be a failed outburst. Between 2008 and 2012, three outbursts were reported by Zhou et al. (2013) [21]. Zhou et al. (2013) compared the timing and spectral evolution on the failed and completed outbursts. They constrained a region for the spectral transitions to HSS for the two outbursts in HID diagrams [21,22]. Since RXTE was decommissioned formally on January 5, 2012, the outburst in 2011 was the last one recorded by RXTE for H 1743-322 [3].

The 2005 outburst of H 1743-322 is a short and faint one, where the peak luminosity $L_{3-25\text{keV,peak}} \sim 0.03 L_{\text{Edd}}$. The faint outburst might underlay the microphysics of BH XRBs [12]. Due to the lower X-ray luminosity, the outburst has not been detail reported in past work. To explore the physical mechanism of faint outburst, we will present the X-ray spectral and timing analysis of H 1743-322 during its 2005 outburst. The paper is organized as follows: in Section 2, we describe the data reduction and analyses procedures. The results of X-ray spectral and timing analyses are presented in Section 3, which are discussed in Section 4 and summarized in Section 5.

2. Data Reduction and Analysis

In this paper, all of the 22 observations of H 1743-322 are from the Proportional Counter Array (PCA) on the RXTE [23]. Since the PCU 2 is the best calibrated detector among five PCUs, we only selected the top layer of the Proportional Counter Unit 2 (PCU 2) from standard 2 data. The standard procedures described in the RXTE cookbook were followed for the data reduction with HEASoft v6.28 [24].

The total photon count rates were first extracted after the deduction of the background and the hardness ratios (HR) were calculated by the formula $HR = C/A$, where the A and C are the net counts rate in 3–5 keV and 5–12 keV energy band, respectively. The X-ray spectra were also extracted with the top layer of PCU 2 from standard 2 data [25]. The response matrices were created by the ftool pcarsp and the background spectra were generated by the ftool pcabackest with the latest PCA background model (faint or bright) according to brightness level. The X-ray spectra and background spectra were generated with the ftool saextract.

To explore the X-ray spectral properties of H 1743-322 during the 2005 outburst, we analyzed the X-ray data in 3–60 keV energy band with XSPEC V12.11.1 [26]. When we analyzed the X-ray spectra, the simplest model possible was adopted. We used an absorbed component (*Phabs*) and power-law (*Powerlaw*) as a beginning model, where the hydrogen column density was frozen as $N_{\text{H}} = 1.6 \times 10^{22} \text{ cm}^{-2}$ and systematic error was fixed at 0.5% [27,28]. The new components (e.g., a multi-temperature disk black-body component (*Diskbb*) and/or Gauss emission line (*Gau*, fixed at 6.4 keV)) were considered if the components can greatly improve the fitting results ($\Delta\chi^2 > 0.3$). We also analyzed the temporal properties of H 1743-322 during the 2005 outburst. The root means square (*rms*) was calculated with the formula $rms = 100 \times \sqrt{WN\pi/2}$, where *W* is the full width at half-maximum of the Lorentzian, and *N* is the Miyamoto normalization of the Lorentzian [29–32]. The uncertainties were obtained by varying the parameters until $\Delta\chi^2 \sim 1$ at 1σ level. The observational ID, disk temperature (T_{in}), photon index (Γ), inner radius (R_{in}), 3–25 keV X-ray flux ($F_{3-25\text{keV}}$), luminosity ratio ($\frac{L_{3-25\text{keV}}}{L_{\text{Edd}}}$), the ratio of the fitted power-law component to the total flux (FLR), *rms*, QPOs, χ^2 and adopted models were shown in Tables 1 and 2.

Table 1. The best fitting parameters of the spectra of H1743-322 during the “faint” 2005 outburst.

Obs.Id (day)	T_{in} (keV)	Γ	R_{in} (R_g)	$F_{3-25\text{keV}}$ ($10^{-9}\text{erg} \cdot \text{cm}^{-2} \cdot \text{s}^{-1}$)	$\text{Log } \frac{L_{3-25\text{keV}}}{L_{\text{Edd}}}$	FLR (%)	$\chi^2/\text{d.o.f}$	Model
91050-06-01-00	$0.92^{+0.05}_{-0.05}$	$2.21^{+0.04}_{-0.04}$	$1.40^{+0.02}_{-0.02}$	$3.41^{+0.03}_{-0.03}$	−1.73	78.58	0.55/82	diskbb+gau+pow
91050-06-02-00	$0.88^{+0.02}_{-0.02}$	$2.15^{+0.03}_{-0.02}$	$3.51^{+0.03}_{-0.02}$	$3.73^{+0.05}_{-0.03}$	−1.69	44.79	0.70/82	diskbb+gau+pow
91050-06-03-00	$0.82^{+0.01}_{-0.01}$	$2.28^{+0.03}_{-0.03}$	$2.96^{+0.02}_{-0.02}$	$3.89^{+0.07}_{-0.05}$	−1.67	49.26	1.26/84	diskbb+pow
91050-06-04-00	$1.02^{+0.01}_{-0.01}$	$2.27^{+0.02}_{-0.02}$	$2.31^{+0.02}_{-0.02}$	$5.57^{+0.03}_{-0.04}$	−1.51	65.38	1.07/84	diskbb+pow
91050-06-05-00	$0.87^{+0.01}_{-0.01}$	$2.33^{+0.06}_{-0.06}$	$3.61^{+0.02}_{-0.04}$	$3.20^{+0.03}_{-0.03}$	−1.75	40.01	0.75/84	diskbb+pow
91050-06-06-00	$0.87^{+0.01}_{-0.01}$	$2.38^{+0.04}_{-0.04}$	$3.35^{+0.06}_{-0.07}$	$3.12^{+0.06}_{-0.04}$	−1.76	48.91	1.29/84	diskbb+pow
91050-06-07-00	$0.83^{+0.02}_{-0.02}$	$2.29^{+0.06}_{-0.05}$	$4.10^{+0.06}_{-0.04}$	$2.54^{+0.03}_{-0.04}$	−1.85	31.02	1.30/84	diskbb+pow
91050-06-08-00	$0.82^{+0.01}_{-0.01}$	$2.21^{+0.05}_{-0.05}$	$3.61^{+0.02}_{-0.04}$	$2.50^{+0.09}_{-0.08}$	−1.86	46.77	0.83/82	diskbb+gau+pow
91050-06-09-00	$0.82^{+0.01}_{-0.01}$	$2.19^{+0.02}_{-0.05}$	$3.57^{+0.02}_{-0.02}$	$2.35^{+0.09}_{-0.09}$	−1.88	44.44	0.76/82	diskbb+gau+pow
91050-06-10-00	$0.78^{+0.07}_{-0.07}$	$2.23^{+0.05}_{-0.05}$	$3.87^{+0.03}_{-0.02}$	$2.14^{+0.06}_{-0.08}$	−1.93	42.71	0.76/82	diskbb+gau+pow
91050-06-11-00	$0.78^{+0.02}_{-0.02}$	$2.36^{+0.10}_{-0.06}$	$3.51^{+0.06}_{-0.07}$	$1.92^{+0.07}_{-0.09}$	−1.97	48.43	1.33/84	diskbb+pow
91428-01-02-00	$0.62^{+0.03}_{-0.03}$	$2.41^{+0.03}_{-0.04}$	$4.16^{+0.03}_{-0.03}$	$1.02^{+0.07}_{-0.06}$	−2.25	60.08	1.48/84	diskbb+pow
91428-01-02-01	$0.79^{+0.08}_{-0.05}$	$1.96^{+0.04}_{-0.04}$	$1.03^{+0.02}_{-0.02}$	$0.98^{+0.10}_{-0.09}$	−2.26	89.20	0.72/82	diskbb+gau+pow
91428-01-03-00		$1.87^{+0.01}_{-0.01}$		$0.85^{+0.03}_{-0.02}$	−2.33	100.0	1.11/86	pow
91428-01-03-01		$1.79^{+0.03}_{-0.03}$		$0.46^{+0.02}_{-0.03}$	−2.59	100.0	1.00/86	pow
91428-01-04-00		$1.88^{+0.03}_{-0.03}$		$0.26^{+0.03}_{-0.03}$	−2.84	100.0	1.22/86	pow
91428-01-04-01		$1.96^{+0.04}_{-0.04}$		$0.21^{+0.03}_{-0.02}$	−2.94	100.0	1.25/86	pow
91428-01-05-00		$2.13^{+0.05}_{-0.05}$		$0.14^{+0.03}_{-0.03}$	−3.13	100.0	1.28/86	pow
91428-01-05-01		$2.26^{+0.07}_{-0.07}$		$0.12^{+0.02}_{-0.03}$	−3.19	96.84	0.80/84	gau+pow
91428-01-06-00		$2.25^{+0.07}_{-0.07}$		$0.11^{+0.03}_{-0.03}$	−3.21	97.51	1.02/84	gau+pow
91428-01-07-00		$2.19^{+0.07}_{-0.07}$		$0.11^{+0.03}_{-0.02}$	−3.24	100.0	1.29/86	pow
91428-01-08-00		$2.22^{+0.07}_{-0.07}$		$0.10^{+0.01}_{-0.02}$	−3.26	100.0	1.14/86	pow

Table 2. The best fitting parameters of the timing of H 1743-322 during the “faint” 2005 outburst.

Obs.Id	rms (%)	QPOs (Hz)	χ^2	Model ¹
91050-06-01-00	13.06	$6.09^{+0.04}_{-0.04}$	0.982	lo
91050-06-02-00	13.79		0.964	lo+pow
91050-06-03-00	4.892		0.924	lo+pow
91050-06-04-00	8.174		1.113	lo+pow
91050-06-05-00	5.005		1.257	lo
91050-06-06-00	9.023		1.088	lo
91050-06-07-00	4.021		0.997	lo
91050-06-08-00	2.688		0.865	lo+pow
91050-06-09-00	3.022		0.873	lo+pow
91050-06-10-00	5.430		0.881	lo+pow
91050-06-11-00	2.401		1.222	lo
91428-01-02-00	4.062	$4.18^{+0.04}_{-0.04}$ $1.84^{+0.05}_{-0.04}$	1.311	lo
91428-01-02-01	11.45		1.006	lo
91428-01-03-00	25.63		0.994	lo+pow
91428-01-03-01	24.52		0.917	lo
91428-01-04-00	25.14		0.994	lo
91428-01-04-01	26.94		0.903	lo+pow
91428-01-05-00	20.94		0.824	lo+pow
91428-01-05-01	27.55		0.715	lo+pow
91428-01-06-00	11.73		0.779	lo
91428-01-07-00	17.51		0.843	lo
91428-01-08-00	16.55		0.799	lo

¹ lo represents the Lorenz function and pow represents the powerlaw function.

3. Results

In this section, we presented the results obtained from its X-ray timing and spectral analysis. In our fitting, we froze the hydrogen column density as $N_H = 1.6 \times 10^{22} \text{ cm}^{-2}$ and assumed the iron emission line at 6.4 keV. The reduced chi-squares cover the range of 0.55 to 1.48. The main fitting parameters were shown in Tables 1 and 2, and Figures 1–7.

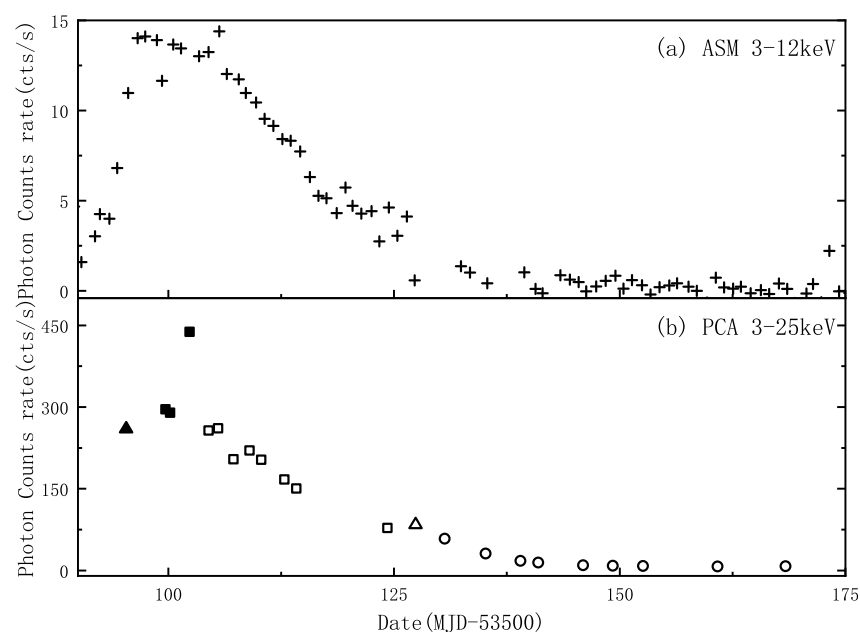


Figure 1. The light curve of H 1743-322 during the “faint” 2005 outburst. (a) The observations from RXTE/ASM; (b) The observations from RXTE/PCA. The filled and open points represent the observations in the rising phase and the decay phase, respectively. The triangles, squares, and circles represent IMS, HSS and LHS, respectively.

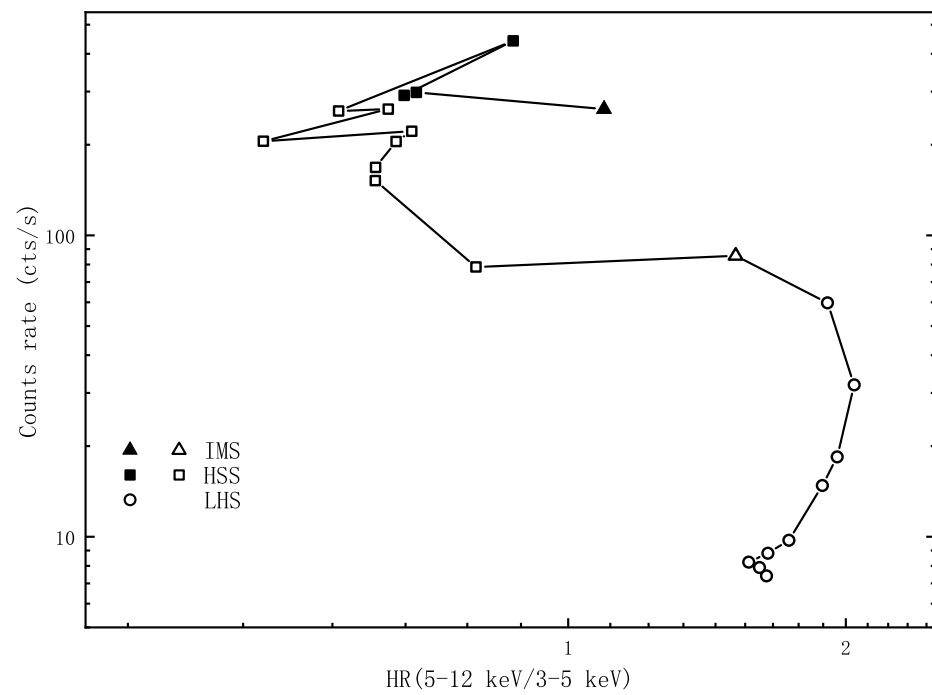


Figure 2. The HID of H 1743-322 during the “faint” 2005 outburst. The symbol types are the same as Figure 1.

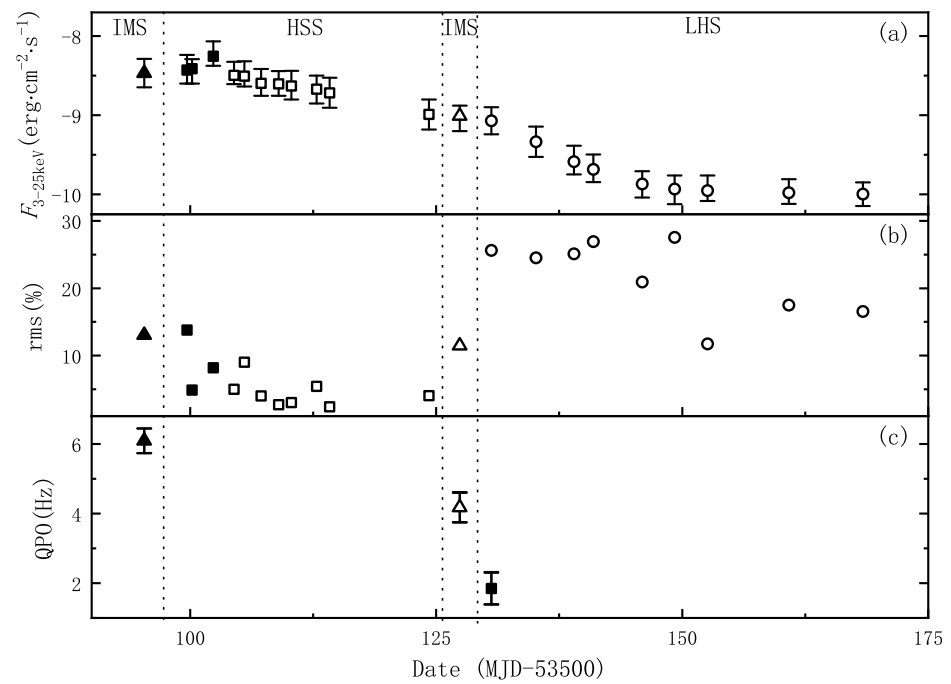


Figure 3. The evolution of 3–25 keV X-ray flux, *rms* and QPOs of H 1743-322 during the “faint” 2005 outburst. The symbol types are the same as Figure 1.

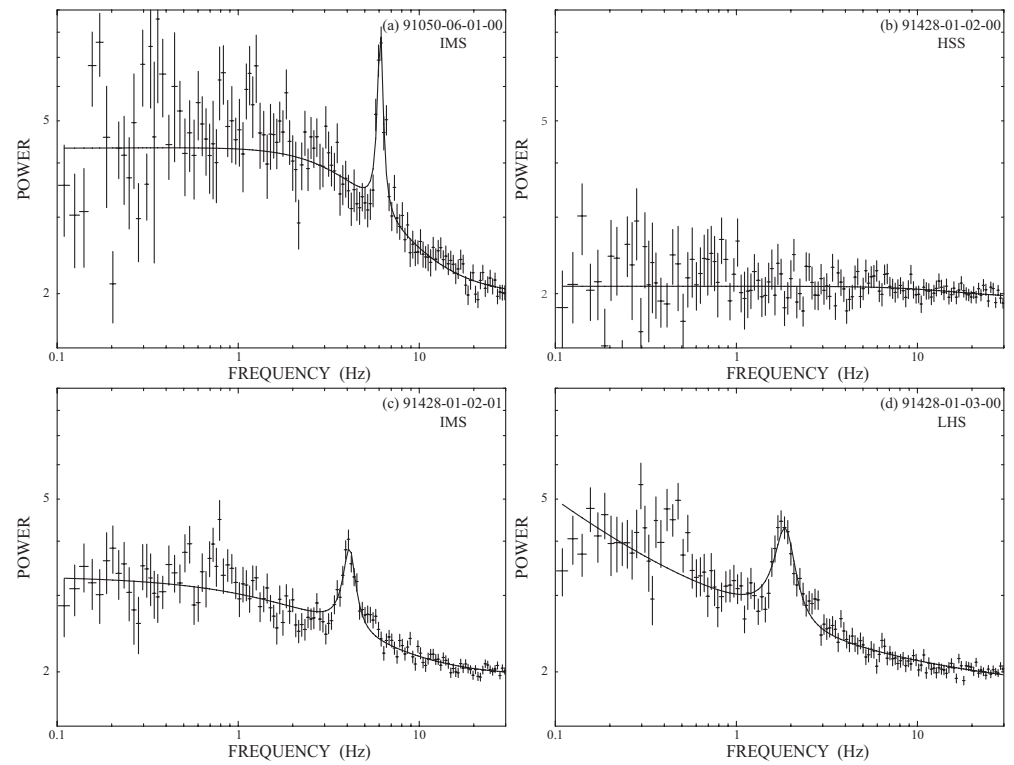


Figure 4. The power density spectra of H 1743-322 among LHS, HSS and LHS.

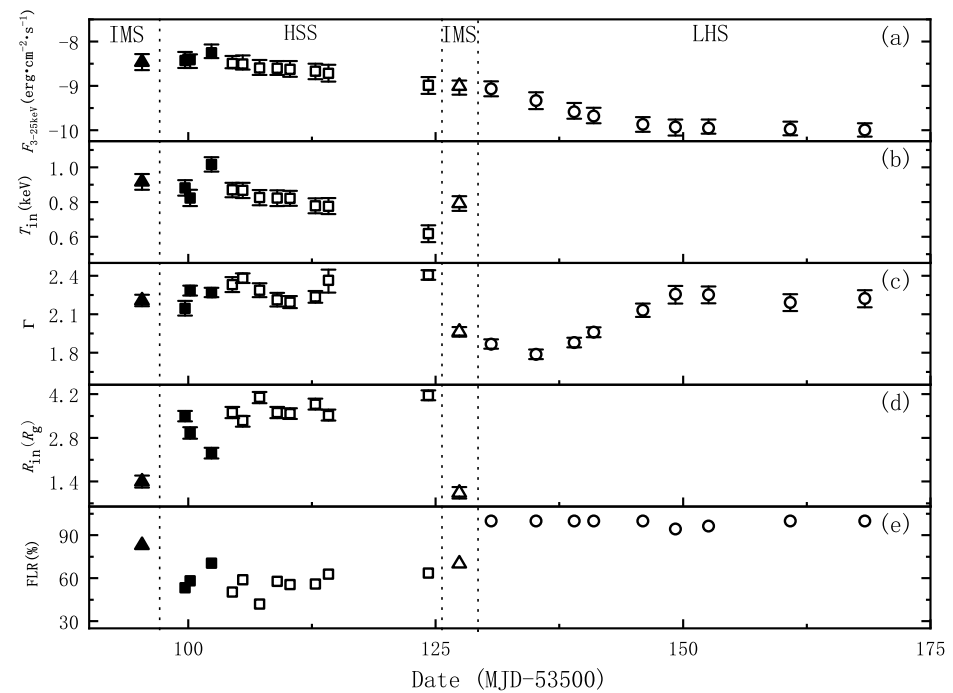


Figure 5. The evolution of spectral fitted parameters of H 1743-322 during the “faint” 2005 outburst. (a) the 3–25 KeV X-ray flux $F_{3-25\text{keV}}$; (b) the inner disk temperature T_{in} ; (c) the spectral index Γ ; (d) the inner radius of accretion disk R_{in} ; (e) the ratio of the fitted power-law component to the total flux FLR. The symbol types are the same as Figure 1.

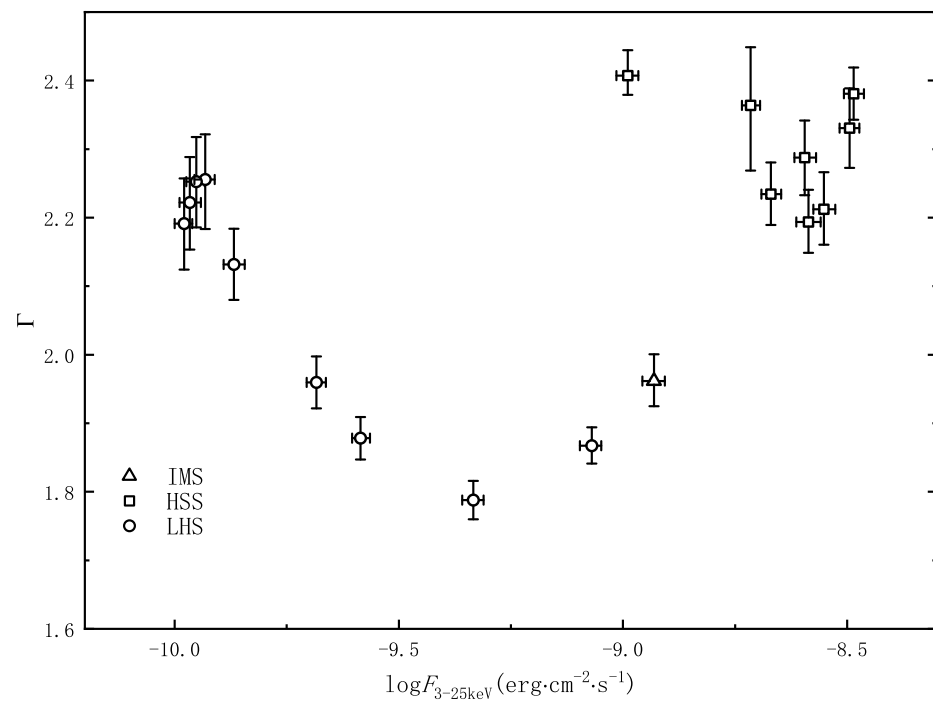


Figure 6. The correlation between the spectral index Γ and the X-ray flux, $F_{3-25\text{keV}}$ of H 1743-322 during the 2005 outburst. The symbol types are the same as Figure 1.

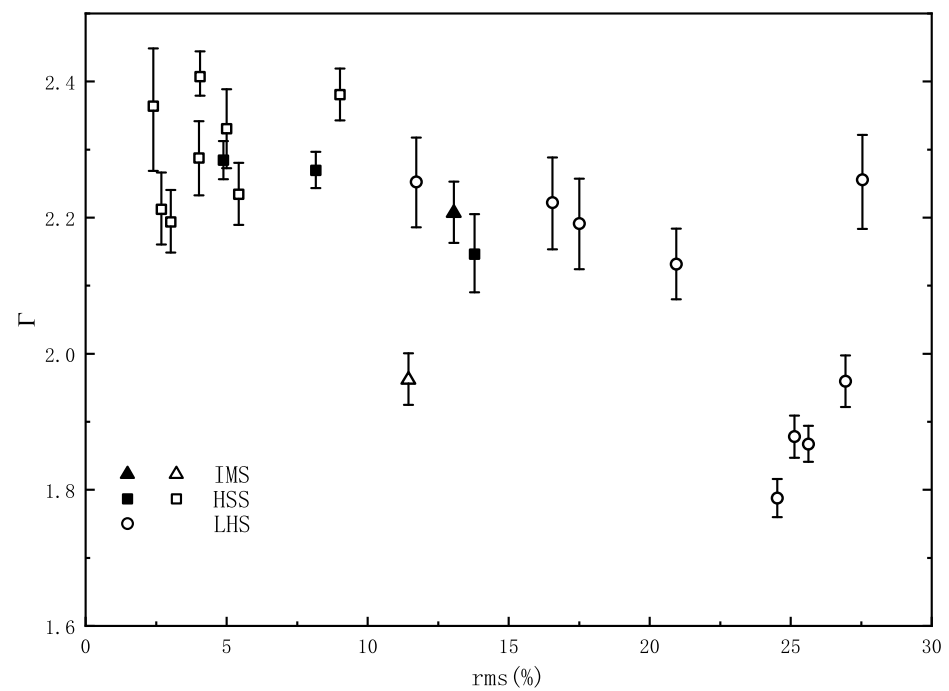


Figure 7. The relation between rms and Γ of H1743-322 during the 2005 outburst. The symbol types are the same as Figure 1.

3.1. Timing Analysis

In Figure 1, we presented the X-ray light curve of H 1743-322 during the 2005 outburst. The top panel and the second panel showed the light curve in 3–12 keV (RXTE/ASM) and 3–25 keV (RXTE/PCA), respectively, where state transitions were observed. Similar results were also observed in other outbursts of H 1743-322 and other sources [13,33].

The HID of H 1743-322 was shown in Figure 2, which covered 22 RXTE/PCA observations and only 4 observational points were in the rising phase. In Figure 3 and Table 2, we represented the best-fitting parameters of X-ray timing of H 1743-322 during the 2005 outburst. We can find that the values of the total fractional rms and the central frequency of LFQPO are $rms \sim 13.06\%$ and $\nu \sim 6.09 \pm 0.04$ Hz, which implies the first observation was in the IMS. Soon afterward, H 1743-322 moved horizontally to left into the softer region. In this phase, the rms values were much lower ($rms \sim 10\%$), the QPOs were absent and hardness ratios peak at ~ 0.5 , which implies that H 1743-322 has transitioned into HSS. Then, H 1743-322 moved horizontally to right and gradually returned into LHS. Therefore, the 2005 outburst of H 1743-322 is a normal one, although its HID is not a full q-like pattern.

To explore the timing properties of H 1743-322, we further showed four typical PDS among IMS, HSS and LHS in Figure 4. The PDS of the top-left panel (Obs.Id: 91050-06-01-00) shows a significant feature with a flat-top noise (red noise) plus a QPO peak (see Figure 4a), which implies the point in HIMS. The PDS of top-right panel (Obs.Id: 91428-01-02-00) has not a QPO signal, which implies the point in HSS. Similar to the top-left panel, the bottom-left panel (Obs.Id: 91428-01-02-01) also shows a flat-top noise, which implies that H 1743-322 has returned to HIMS. The bottom-right panel (Obs.Id: 91428-01-03-00) belongs to LHS because of the lack of red noise in its PDS.

3.2. Spectral Analysis

The best-fitting parameters of the X-ray spectra of H 1743-322 during the 2005 outburst were shown in Figure 5. The first X-ray observation can be well fitted with the model $pha(diskbb + gau + powerlaw)$. The main fitting parameters (e.g., $T_{in} = 0.92 \pm 0.04$ keV, $\Gamma = 2.21 \pm 0.04$, $R_{in} = 1.40 \pm 0.02 R_g$ and FLR $\sim 78.58\%$) indicated that H 1743-322 is in IMS. Then, the FLR shows a sharp decrease and the contribution of the power-law component to total flux is less than 60%, which implies H 1743-322 has entered into HSS between MJD = 53599–53624. In this state, the inner accretion disk temperature T_{in} , the photon index and the inner radius of accretion disk show a little change, that is, $T_{in} \sim 0.6–1.0$ keV, $\Gamma \sim 2.1–2.4$ and $R_{in} \sim 2.3–4.2 R_g$. Right after HSS, H 1743-322 transitioned into IMS and LHS again. It is obvious that the fitting parameters also undergo a great change during the transitions from HSS to IMS and from IMS to LHS.

3.3. Relation of Timing and Spectral Properties

In this section, we related the timing properties and the spectral properties. We first explored the evolution of X-ray spectral index, Γ , on the 3–25 keV X-ray flux, $F_{3-25keV}$. On account of the fewer observations, it is difficult to investigate the X-ray spectral evolution in the rising phase. Therefore, we only explored the $F_{3-25keV} - \Gamma$ correlation in the decay phase (see Figure 6). It is obvious that the X-ray spectral evolution in the decay phase can be divided into three stages. In the first stage, the spectral index shows a shallower positive correlation, where the spectral index changes a little. According to the timing and spectral properties (see Tables 1 and 2), H 1743-322 was in HSS at this stage. With the further decrease of the X-ray flux, the X-ray spectra of H 1743-322 quickly harden, where the $F_{3-25keV} - \Gamma$ correlation roughly follows a positive correlation. It should be noted that the positive $F_{3-25keV} - \Gamma$ correlation was very obvious even though only two observations at this stage. The $F_{3-25keV} - \Gamma$ correlation became negative, when X-ray flux, $F_{3-25keV}$, was lower than a critical value $F_{X,crit} \sim 4.64 \times 10^{-10} \text{ erg} \cdot \text{cm}^{-2} \cdot \text{s}^{-1}$, corresponding X-ray luminosity $L_{3-25keV} \sim 2.55 \times 10^{-3} L_{Edd}$.

To detail learn about the timing evolution on the spectral properties, we further explored the relation between the total fractional rms and the X-ray spectral photon Γ (see Figure 7). It can be clearly found that the relation of $rms - \Gamma$ displays a linear, negative correlation. The tight correlation implies a similar physical mechanism between the QPOs and spectral shape. The similar correlations between X-ray timing and spectrum were also reported in other sources [34]. In a word, the spectral parameters seem to follow the timing behavior, which is expected in normal state transition during outbursts of black hole X-ray binary [26].

4. Discussion

In this paper, we have performed the timing and spectral analysis of H 1743-322 during the faint 2005 outburst with the RXTE/PCA data. The light curves characterized by a fast rise and exponential decay (FRED) and the softening X-ray spectra were observed near the peak flux. Although the fewer observations in the rising phase, H 1743-322 remains a counter-clockwise and q-like pattern in the Hardness-Intensity Diagram like other canonical outbursts [35,36]. During the outburst, H 1743-322 went through a canonical state transition among LHS, IMS and HSS. However, the intrinsic physics behind the HID is still an open question [37,38]. The shape of HIDs might be affected by the inclination and magnetic field of the accretion disk [39].

According to the criterion of mini-outbursts of BH XRBs [13], We think that the faint 2005 outburst is not a mini-outburst but a faint normal outburst. The main reasons are followed as: (1) the time interval between the 2004 outburst and the 2005 outburst $\Delta t \sim 320$ days and displays a full state transition; (2) The ratio between re-brightening peak flux and the normal outburst peak flux $F_i/F_{\text{out}} \sim 0.93 > 0.7$; (3) The ratio of $\Delta t_i/\Delta t_{\text{out}} \sim 2.64 > 1$, where the Δt_i is the time separating the start of the quiescent period from the start of each re-brightening, and Δt_{out} is the duration of the main outburst.

During the faint 2005 outburst, the spectra and timing parameters show a significant change. In particular, the inner disk temperatures gradually decline with the decrease of X-ray flux in HSS, while the inner radius of accretion disk is nearly constant. Since the inner radius of accretion disk is only determined by the BH mass and spin, the constant inner radius implies that the accretion disk extends into the innermost stable circular orbit (ISCO) around the black hole [40–42]. We know that the radius of innermost stable circular orbit of non-rotating black hole $R_{\text{ISCO}} \sim 3 R_g$, where $R_g = \frac{GM_{\text{BH}}}{c^2}$ is the gravitational radius of black hole. Therefore, we conclude that the H 1743-322 is a low-spin black hole, since the inner radius of accretion $R_{\text{in}} \simeq 3.51^{+0.65}_{-1.20} R_g$ (see Table 1 and Figure 5). In addition, compared with the HSS, the contribution of the power-law component to the total flux become higher in IMS (FLR $\simeq 89.20\%$). The other timing and spectral parameters also present a sudden change (see Figure 5). The inner disk temperature and the total fractional *rms* show a sharp rise, while the inner radius and spectral index present a significant decrease in several days. These results suggest that the accretion disk has extended into the innermost stable circular orbit (ISCO) around the black hole and the inverse Compton scatter in the corona becomes stronger in IMS (e.g., [43–46]). It was well known that the temperature of thermal component is determined by the spectral shape and the R_{in} can be calculated from normalization parameters. Therefore, the smaller R_{in} might mean the thermal flux is somewhat lower in IMS.

We also obtain the relation between timing and spectral parameters, using the RXTE/PCA data during the 2005 outburst of H 1743-322. The total fractional *rms* and spectral index shows a roughly linear, negative correlation. Generally speaking, the amount of soft photons from accretion disk seems invariable. Therefore, an increase of the number of soft photons will dilute the variability from the harder photons. In other words, the softer the X-ray spectra, the smaller total fractional *rms*. The evolution of the photon index on the X-ray flux has been found in other BH XRBs and AGNs [47]. During the 2005 outburst, the positive and negative correlation between the photon index Γ and 3–25 keV X-ray flux, $F_{3-25\text{keV}}$, were obtained, and the critical transitioned luminosity between positive and negative correlation $L_{X,\text{crit}} \sim 2.55 \times 10^{-3} L_{\text{Edd}}$ was constrained. These can be well explained by the Shakura-Sunyaev disk-corona model (SSD-corona) and advection-dominated accretion flow (ADAF) [48,49], respectively.

5. Summary

Because the outburst of H 1743-322 in 2005 is a shorter and fainter one, it has not been reported in past work. In this paper, we performed a detailed timing and spectral analysis with the RXTE/PCA data. The main results are summarized as follows: (1) We find that H 1743-322 went through a state transition from the HSS to LHS via IMS like other sources. In

this outburst, the timing and spectral parameters showed a significant change. In particular, the inner radius of the accretion disk in HSS was almost a constant, which was used to constrain $R_{\text{ISCO}} \sim 3.50 R_g$. These imply H 1743-322 is a low-spin black hole. (2) The timing and spectral parameters (e.g., T_{in} , Γ , R_{in} , rms and QPOs, etc.) undergo a great change in several days during the transitions between IMS and HSS, which may correspond to the evolution of the accretion disk and corona [50,51]. (3) The spectral parameters seem to follow the timing behavior (e.g., the relations of $\Gamma - F_{3-25\text{keV}}$ and $\Gamma - rms$), which is expected for the normal outbursts of black hole X-ray binaries.

Author Contributions: Data curation, A.D., C.L. and Q.S.; Formal analysis, A.D., C.L. and Q.Z.; Software, Z.Y., Q.S. and B.D.; Writing—original draft, A.D. and C.L.; writing—review and editing, A.D.; Funding acquisition, A.D. All authors have read and agreed to the published version of the manuscript.

Funding: This work was supported by National Key R&D Program of China (2018YFA0404602), NSFC (U1831120, U1731238), the Foundation of Guizhou Provincial Education Department (2021049, 2021056, (2020)003)), the Excellent Postdoctoral Foundation of Xinjiang and YJSCXJH([2020]096).

Institutional Review Board Statement: Not applicable.

Informed Consent Statement: Not applicable.

Data Availability Statement: <https://heasarc.gsfc.nasa.gov/>.

Acknowledgments: We thank the members of the GZNU astrophysics group for many useful discussions and comments.

Conflicts of Interest: The authors declare no conflict of interest.

References

1. Athulya, M.P.; Radhika, D.; Agrawal, V.K.; Ravishankar, B.T.; Naik, S.; Mandal, S.; Nandi, A. Unravelling the foretime of GRS 1915+105 using AstroSat observations: Wide-band spectral and temporal characteristics. *Mon. Not. R. Astron. Soc.* **2021**, *510*, 3019–3038. [\[CrossRef\]](#)
2. Liu, X.; Chang, N.; Wang, X.; Yuan, Q. The Origin of Radio Emission in Black Hole X-ray Binaries. *Galaxies* **2021**, *9*, 78. [\[CrossRef\]](#)
3. Sriram, K.; Harikrishna, S.; Choi, C.S. Spectro-temporal Studies of Rapid Transition of the Quasi-periodic Oscillations in the Black Hole Source H 1743-322. *Astrophys. J.* **2021**, *911*, 17–56. [\[CrossRef\]](#)
4. Casella, P.; Belloni, T.; Stella, L. The ABC of Low-Frequency Quasi-periodic Oscillations in Black Hole Candidates: Analogies with Z Sources. *Astrophys. J.* **2005**, *629*, 403–407. [\[CrossRef\]](#)
5. Motta, S.E. Quasi periodic oscillations in black hole binaries. *Astron. Nachrichten* **2016**, *337*, 398–404. [\[CrossRef\]](#)
6. Lazar, H.; Tomsick, J.A.; Pike, S.N.; Bachetti, M.; Buisson, D.J.; Connors, R.M.; Fabian, A.C.; Fuerst, F.; García, J.A.; Hare, J.; et al. Spectral and Timing Analysis of NuSTAR and Swift/XRT Observations of the X-Ray Transient MAXI J0637-430. *Astrophys. J.* **2021**, *921*, 14–30. [\[CrossRef\]](#)
7. Yan, Z.; Rapisarda, E.; Yu, W.F. Detection of a Low-frequency Quasi-periodic Oscillation in the Soft State of Cygnus X-1 with Insight-HXMT. *Mon. Not. R. Astron. Soc.* **2021**, *919*, 9–20. [\[CrossRef\]](#)
8. Nathan, E.; Ingram, A.; Homan, J.; Huppenkothen, D.; Uttley, P.; van der Klis, M.; Motta, S.; Altamirano, D.; Middleton, M. Phase-resolved spectroscopy of a quasi-periodic oscillation in the black hole X-ray binary GRS 1915+105 with NICER and NuSTAR. *Mon. Not. R. Astron. Soc.* **2022**, *511*, 255–279. [\[CrossRef\]](#)
9. Motta, S.E.; Casella, P.; Henze, M.; Muñoz-Darias, T.; Sanna, A.; Fender, R.; Belloni, T. Geometrical constraints on the origin of timing signals from black holes. *Mon. Not. R. Astron. Soc.* **2015**, *447*, 2059–2072. [\[CrossRef\]](#)
10. Belloni, T.; Zhang, L.; Kylafis, N.D.; Reig, P.; Altamirano, D. Time lags of the type-B quasi-periodic oscillation in MAXI J1348-630. *Mon. Not. R. Astron. Soc.* **2020**, *496*, 4366–4371. [\[CrossRef\]](#)
11. Yan, Z.; Yu, W.F. Detection of X-ray spectral state transitions in mini-outbursts of black hole transient GRS 1739-278. *Mon. Not. R. Astron. Soc.* **2017**, *470*, 4298–4306. [\[CrossRef\]](#)
12. Xie, F.G.; Yan, Z.; Wu, Z.Z. Radio/X-Ray Correlation in the Mini-outbursts of Black Hole X-Ray Transient GRS 1739-278. *Astrophys. J.* **2020**, *891*, 31–39. [\[CrossRef\]](#)
13. Zhang, G.B.; Bernardini, F.; Russell, D.M.; Gelfand, J.D.; Lasota, J.P.; Qasim, A.A.; AlMannaei, A.; Koljonen, K.I.I.; Shaw, A.W.; Lewis, F.; et al. Bright Mini-outburst Ends the 12 yr Long Activity of the Black Hole Candidate Swift J1753.5-0127. *Astrophys. J.* **2019**, *876*, 5–16. [\[CrossRef\]](#)
14. Hynes, R.I.; Mauche, C.W.; Haswell, C.A.; Shrader, C.R.; Cui, W.; Chaty, S. The X-Ray Transient XTE J1118+480: Multiwavelength Observations of a Low-State Minioutburst. *Astrophys. J.* **2000**, *539*, L37–L40. [\[CrossRef\]](#)

15. Dubus, G.; Hameury, J.M.; Lasota, J.P. The disc instability model for X-ray transients: Evidence for truncation and irradiation. *Astron. Astrophys.* **2001**, *373*, 251–272. [\[CrossRef\]](#)
16. Hameury, J.M.; Lasota, J.P.; Warner, B. The zoo of dwarf novae: Illumination, evaporation and disc radius variation. *Astron. Astrophys.* **2000**, *353*, 244–253.
17. Cooke, B.A.; YLevine, A.M.; Lang, F.L.; Primini, F.A.; Lewin, W.H.G. HEAO 1 high-energy X-ray observations of three bright transient X-ray sources H 1705-250 (nova Ophiuchi), H 1743-322 and H 1833-077 (Scutum X-1). *Astrophys. J.* **1984**, *285*, 258–263. [\[CrossRef\]](#)
18. Reynolds, S.P.; Chanan, G.A. On the X-ray emission from Crab-like supernova remnants. *Astrophys. J.* **1984**, *281*, 673–681. [\[CrossRef\]](#)
19. Steiner, J.F.; McClintock, J.E.; Reid, M.J. The Distance, Inclination, and Spin of the Black Hole Microquasar H 1743-322. *Astrophys. J.* **2012**, *745*, L7–L11. [\[CrossRef\]](#)
20. Bhattacharjee, A.; Banerjee, I.; Banerjee, A.; Debnath, D.; Chakrabarti, S.K. The 2004 outburst of BHC H 1743-322: Analysis of spectral and timing properties using the TCAF solution. *Mon. Not. R. Astron. Soc.* **2017**, *466*, 1372–1381. [\[CrossRef\]](#)
21. Zhou, J.N.; Liu, Q.Z.; Chen, Y.P.; Li, J.; Qu, J.L.; Zhang, S.; Gao, H.Q.; Zhang, Z. The last three outbursts of H 1743-322 observed by RXTE in its latest service phase. *Mon. Not. R. Astron. Soc.* **2013**, *431*, 2285–2293. [\[CrossRef\]](#)
22. Belloni, T.; Motta, S.E.; Muñoz, D.T. Black hole transients. *Bull. Astron. Soc. India* **2011**, *39*, 409–428.
23. Markwardt, C.B.; Swank, J.H. XTE J1746-322 = Igr J17464-3213 = H 1743-322. *Astron. Telegr.* **2003**, *133*, 1–24.
24. Mao, D.M.; Yu, W.F. Power spectral properties of the soft spectral states in four black hole transients. *Res. Astron. Astrophys.* **2021**, *21*, 12–25. [\[CrossRef\]](#)
25. Cao, X.F.; Wu, Q.W.; Dong, A.J. Different X-ray spectral evolution for black hole X-ray binaries in dual tracks of radio-X-ray correlation. *Astrophys. J.* **2014**, *788*, 52–60. [\[CrossRef\]](#)
26. Dong, A.J.; Liu, C.; Ge, K.; Liu, X.; Zhi, Q.J.; You, Z.Y. A Study on the Hysteresis Effect and Spectral Evolution in the Mini-Outbursts of Black Hole X-Ray Binary XTE J1550-564. *Front. Astron. Space Sci.* **2021**, *8*, 37–43. [\[CrossRef\]](#)
27. Motta, S.E.; Darias, T.M.; Belloni, T. On the outburst evolution of H 1743-322: A 2008/2009 comparison. *Mon. Not. R. Astron. Soc.* **2010**, *408*, 1796–1807. [\[CrossRef\]](#)
28. Magdziarz, P.; Zdziarski, A.A. Angle-dependent Compton reflection of X-rays and gamma-rays. *Mon. Not. R. Astron. Soc.* **1995**, *273*, 837–848. [\[CrossRef\]](#)
29. Miyamoto, S.; Kitamoto, S.; Iga, S.; Negoro, H.; Terada, K. Canonical Time Variations of X-Rays from Black Hole Candidates in the Low-Intensity State. *Astrophys. J.* **1992**, *391*, L21–L24. [\[CrossRef\]](#)
30. Vaughan, S.; Fabian, A.C. The high frequency power spectrum of Markarian 766. *Astrophys. J.* **2003**, *341*, 496–500. [\[CrossRef\]](#)
31. Berger, M. High time resolution observations of Cygnus X-3 with EXOSAT. *Astron. Astrophys.* **1994**, *292*, 175–182.
32. Rodriguez, J.; Varnière, P. The Puzzling Harmonic Behavior of the Cathedral QPO in XTE J1859+226. *Astrophys. J.* **2011**, *735*, 79–85. [\[CrossRef\]](#)
33. Miller-Jones, J.C.; Sivakoff, G.R.; Altamirano, D.; Coriat, M.; Corbel, S.; Dhawan, V.; Krimm, H.A.; Remillard, R.A.; Rupen, M.P.; Russell, D.M.; et al. Disc-jet coupling in the 2009 outburst of the black hole candidate H 1743-322. *Mon. Not. R. Astron. Soc.* **2012**, *412*, 468–485.
34. Shui, Q.C.; Yin, H.X.; Zhang, S.; Qu, J.L.; Chen, Y.P.; Kong, L.D.; Wang, P.J.; Zhang, H.F.; Song, J.X.; Ning, B.; et al. State transitions of GX 339-4 during its outburst rising phase. *Mon. Not. R. Astron. Soc.* **2021**, *508*, 287–299. [\[CrossRef\]](#)
35. Marcel, G.; Ferreira, J.; Petrucci, P.O.; Belmont, R.; Malzac, J.; Clavel, M.; Henri, G.; Coriat, M.; Corbel, S.; Rodriguez, J.; et al. A unified accretion-ejection paradigm for black hole X-ray binaries. VI. Radiative efficiency and radio-X-ray correlation during four outbursts from GX339-4. *Astron. Astrophys.* **2021**, *494*, L21–L24.
36. Belloni, T.; Parolin, I.; Del Santo, M.; Homan, J.; Casella, P.; Fender, R.P.; Lewin, W.H.G.; Méndez, M.; Miller, J.M.; Van Der Klis, M. INTEGRAL/RXTE high-energy observation of a state transition of GX339-4. *Mon. Not. R. Astron. Soc.* **2006**, *367*, 1113–1120. [\[CrossRef\]](#)
37. McClintock, J.E.; Remillard, R.A. Black Hole X-ray Binaries. *Astron. Astrophys.* **2004**, *3*, 1–58.
38. Zhang, S.N. Black hole binaries and microquasars. *Front. Phys.* **2013**, *8*, 630–660. [\[CrossRef\]](#)
39. Mosallanezhad, A.; Abbassi, S.; Beiranv, N. Structure of Advection-Dominated Accretion Disks with Outflows: Role of Toroidal Magnetic Field. *Mon. Not. R. Astron. Soc.* **2014**, *437*, 3112–3123. [\[CrossRef\]](#)
40. Reynolds, C.S. Observational Constraints on Black Hole Spin. *Astron. Astrophys.* **2020**, *59*, 35–76. [\[CrossRef\]](#)
41. Gao, Z.F.; Shan, H.; Wang, H. The dissipation of toroidal magnetic fields and spin down evolution of young and strongly magnetized pulsars. *Astron. Nachrichten* **2021**, *342*, 369–376. [\[CrossRef\]](#)
42. Gao, Z.F.; Peng, F.K.; Wang, N. The evolution of magnetic field and spin-down of young pulsars. *Astron. Nachrichten* **2019**, *340*, 1023–1029. [\[CrossRef\]](#)
43. Liu, H.; Dong, A.J.; Weng, S.S.; Wu, Q.W. Evolution of the hard X-ray photon index in black-hole X-ray binaries: Hints for accretion physics. *Mon. Not. R. Astron. Soc.* **2019**, *487*, 5335–5345. [\[CrossRef\]](#)
44. Dong, A.J.; Wu, Q.W.; Cao, X.F. A new fundamental plane for radiatively efficient black-hole sources. *Astrophys. J.* **2014**, *787*, 20–25. [\[CrossRef\]](#)
45. Cao, X.W. An accretion disc-corona model for X-ray spectra of active galactic nuclei. *Mon. Not. R. Astron. Soc.* **2009**, *394*, 207–213. [\[CrossRef\]](#)

-
46. Schnittman, J.D.; Krolik, J.H. X-ray Polarization from Accreting Black Holes: Coronal Emission. *Astrophys. J.* **2010**, *712*, 908–924. [[CrossRef](#)]
 47. Liu, X.; Han, Z.H.; Zhang, Z. The physical fundamental plane of black hole activity. *Astrophys. Space Sci.* **2016**, *361*, 9–14. [[CrossRef](#)]
 48. Chang, N.; Xie, F.G.; Liu, X.; Ho, L.C.; Dong, A.J.; Han, Z.H.; Wang, X. Possible evidence of a universal radio/X-ray correlation in a near-complete sample of hard X-ray selected seyfert galaxies. *Mon. Not. R. Astron. Soc.* **2021**, *503*, 1987–1998. [[CrossRef](#)]
 49. Xu, Y.; Harrison, F.A.; Tomsick, J.A.; Hare, J.; Fabian, A.C.; Walton, D.J. Evidence for Disk Truncation at Low Accretion States of the Black Hole Binary MAXI J1820+070 Observed by NuSTAR and XMM-Newton. *Astrophys. J.* **2020**, *893*, 8–15. [[CrossRef](#)]
 50. Li, L.X.; Zimmerman, E.R.; Narayan, R.; McClintock, J.E. Multitemperature Blackbody Spectrum of a Thin Accretion Disk Around a Kerr Black Hole: Model Computations and Comparison with Observations. *Astrophys. J.* **2005**, *157*, 335–370. [[CrossRef](#)]
 51. Prieto, A.; Rodríguez-Ardila, A.; Panda, S.; Marinello, M. Erratum: A novel black hole mass scaling relation based on coronal gas, and its dependence with the accretion disc. *Mon. Not. R. Astron. Soc.* **2022**, *511*, 4444–4446. [[CrossRef](#)]